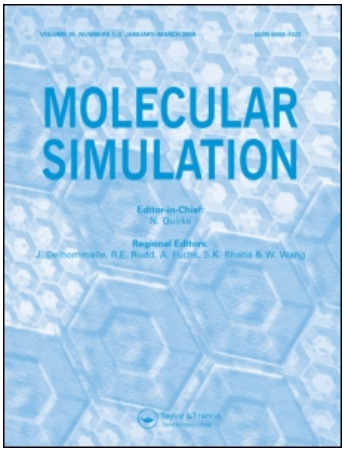

Molecular Simulation
Publication details, including instructions for authors and subscription information:
http://www.informaworld.com/smpp/title~content=t713644482

Molecular simulations of phosphonium-based ionic liquid

Xiaomin Liu[a]; Guohui Zhou[ab]; Suojiang Zhang[a]; Guangren Yu[c]
[a] State Key Laboratory of Multiphase Complex Systems, Institute of Process Engineering, Chinese Academy of Sciences, Beijing, People's Republic of China [b] Beijing Shengjinqiao Information Technology Co., Ltd., Beijing, People's Republic of China [c] College of Chemical Engineering, Beijing University of Chemical Technology, Beijing, People's Republic of China

First published on: 27 August 2009

To cite this Article Liu, Xiaomin , Zhou, Guohui , Zhang, Suojiang and Yu, Guangren(2010) 'Molecular simulations of phosphonium-based ionic liquid', Molecular Simulation, 36: 1, 79 — 86, First published on: 27 August 2009 (iFirst)
To link to this Article: DOI: 10.1080/08927020903124569
URL: http://dx.doi.org/10.1080/08927020903124569

Molecular Simulation
Vol. 36, No. 1, January 2010, 79–86

Taylor & Francis
Taylor & Francis Group

Molecular simulations of phosphonium-based ionic liquid

Xiaomin Liu[a], Guohui Zhou[ab], Suojiang Zhang[a]* and Guangren Yu[c]

[a]*State Key Laboratory of Multiphase Complex Systems, Institute of Process Engineering, Chinese Academy of Sciences, 100190 Beijing, People's Republic of China;* [b]*Beijing Shengjinqiao Information Technology Co., Ltd., 100083 Beijing, People's Republic of China;* [c]*College of Chemical Engineering, Beijing University of Chemical Technology, 100029 Beijing, People's Republic of China*

(*Received 19 March 2009; final version received 16 June 2009*)

Compared with imidazolium-based ionic liquids (ILs), phosphonium-based ILs have been proven to be more stable in thermodynamics and less expensive to manufacture. In this work, a kind of phosphonium-based IL, $[PC_6C_6C_6C_{14}][Tf_2N]$, was studied under several conditions using molecular dynamics simulations based on both the all-atom force field (AAFF) and the united-atom force field. Liquid density was calculated to validate the force field. Compared with experimental data, good agreement was obtained for the simulated density based on the AAFF. Heat capacities at constant pressure were calculated at several temperatures, and good linear relationships were observed. Self-diffusion coefficients, viscosities and conductivities were also calculated to study the dynamics properties of this IL. The viscosity of this IL at 293 K was also compared with experimental data, and the error was in a reasonable range. In order to depict the microstructures of the IL, centre-of-mass and site-to-site radial distribution functions were employed. In addition, spatial distribution functions were investigated to present the more intuitive features.

Keywords: molecular dynamics simulation; ionic liquid; force field

1. Introduction

Ionic liquids (ILs) have attracted much attention due to their peculiar chemical and physical properties [1–9]. In order to develop innovative processes using ILs, two aspects have to be urgently considered. The first is the need to synthesise more task-specific ILs to capture the industrial demands, which is the foundation for studying ILs. More and more kinds of ILs emerge. Although fewer than 100 kinds of ILs were reported in the year 1995, and about 300 kinds of ILs were synthesised in 2000, more than 1800 kinds of ILs have now been reported [10]. The second aspect is the need to understand the structures of this medium. Although ILs have become one of the research hotspots in both the academy and industry, many basic rules are not clear. Understanding the nature of ILs attracts much attention, and there are many challenges on the road to discovery. Any process in this scope will bring revolutionary development for ILs in both chemistry and chemical engineering [11].

ILs are a new kind of solvent with many exciting properties such as negligible vapour pressure, large liquid range, high thermal stability, high ionic conductivity, large electrochemical window and the ability to solvate compounds of widely varying polarity [3,12]. Because of their tempting properties, ILs have prompted extensive research [13,14], and the rapid growth of research based on ILs can be seen in Figure 1(a). However, nearly all the attention has been paid to the imidazolium-based ILs, which can be concluded from the classification of papers about ILs published in 2008 (Figure 1(b)). Actually, except for the imidazolium-based ILs, other kinds of ILs have also been proven to have bright and exciting prospects in industrial applications. For example, compared with imidazolium-based ILs, phosphonium-based ILs are proved to be more stable in thermodynamics and less expensive to manufacture [15–18]. It is reported that these ILs 'offer greater practicality and scope than imidazolium ILs and deserve far more consideration as unique reaction media than has been afforded them in the ILs field thus far' [15].

In this work, molecular dynamics simulations were performed for one of the phosphonium-based ILs, named trihexyl(tetradecyl)phosphonium bis(trifluoromethylsulphonyl)imide ($[PC_6C_6C_6C_{14}][Tf_2N]$). Both the all-atom force field (AAFF) and the united-atom force field (UAFF) were employed. Compared with the UAFF, the AAFF was proved to be more effective for reliable results. Influence of temperature on the thermodynamic and transport properties was considered, and simulations were performed at 273, 373, 473 and 573 K, respectively. Good linear relationships were observed with increasing temperatures for liquid density and heat capacities at constant pressure. In addition, self-diffusion coefficients (SDCs), viscosities, and conductivities were calculated to study the dynamics properties of this IL. In order to depict the microstructures, centre-of-mass and site-to-site radial

*Corresponding author. Email: sjzhang@home.ipe.ac.cn

ISSN 0892-7022 print/ISSN 1029-0435 online

DOI: 10.1080/08927020903124569
http://www.informaworld.com

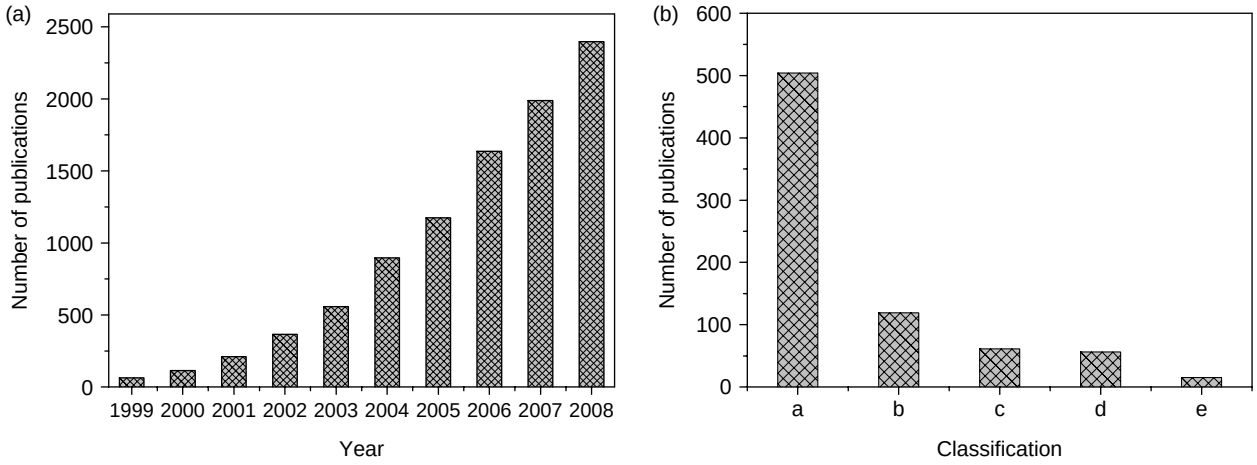

Figure 1. Number of papers containing 'ionic liquids' or 'ionic liquid' in abstract, title and/or keywords according to ISI Web of Science (a) classified by year; and (b) published in 2008 and classified by type of cation: a, imidazolium; b, ammonium; c, pyridinium; d, phosphonium; e, guanidinium-based ILs.

distribution functions (RDFs) were investigated. The spatial distribution functions (SDFs) were also studied to provide more intuitive structures.

2. Molecular dynamics simulation

2.1 Force field

The AAFF provides parameters for every atom in the system, including hydrogen, while the UAFF treats several atoms as a single interaction centre, the most typical example is the hydrogen and carbon atoms in methyl or methylene groups. In this work, both the AAFF and the UAFF were developed in the frame of the AMBER [19] force field for the cation. All the atom types are shown in Figure 2. Force constants for anions were derived directly from the force field developed by Lopes [20]. Parameters for cations including the bonds, angles and torsion force constants were obtained based on our previous work [16]. Optimisation of the isolated ion structures was performed using the Gaussian 03 package at the B3LYP/6-31 + G(d) level. Atom charges were obtained by fitting the electrostatic potential generated calculated at the B3LYP/6-31 + G(d) level, and one conformation, two-steps restraint electrostatic potential method [21–24] was used for atom charges. Van der Waal parameters for phosphorus atoms were based on AMBER and the other parameters for united atoms were derived from optimised potential for liquid simulations force field. All the related parameters are shown in Table S1 in the Supporting information, available online.

2.2 Simulation details

Molecular dynamics simulations were performed using the MDynaMix program, version 5.0 [25]. The simulation system contained 256 pairs of $[PC_6C_6C_6C_{14}][Tf_2N]$. Nose–Hoover NpT ensemble [26] was adopted with the coupling constant of 700 and 100 fs. Two time steps were used with the long and short time steps of 4 and 2 fs, respectively. The glass transition and decomposition temperatures of $[PC_6C_6C_6C_{14}][Tf_2N]$ are 197 and 673 K [17], and simulations were performed at 273, 373, 473 and 573 K, respectively. For each temperature, the equilibrium simulation extended to 400 ps and each production period lasted for 2–4 ns. The configurations of the system were saved for further analyses every five time steps.

3. Results and discussions

3.1 Liquid densities and energy distributions

In this work, the liquid densities of $[PC_6C_6C_6C_{14}][Tf_2N]$ at different temperatures were calculated based on both the AAFF and the UAFF, and the results are shown in Figure 3. It was found that, based on the two force fields, calculated densities decrease linearly with increasing temperature within the range of 300 K. All the AAFF densities are smaller than the corresponding ones based on the UAFF, and that may be caused by the steric effect. It is reported that the experimental density at 293 K is 1.080 g/cm^3 [17]. In order to decide which force field describes the IL more effectively, we carried out the molecular simulation at 293 K. The simulation details are exactly the same as those described in Section 2.2. Although the computed system was effectively reduced from nearly 30,000 atoms to 12,288 interaction sites when we performed calculations based on the UAFF, the AAFF result (1.083 g/cm^3) is proved to be much more reliable compared with the simulation result (1.137 g/cm^3) based on the UAFF. It is reported [27] that density based on the UAFF for [bmim][BF_4] was in good agreement with experimental data; however, $[PC_6C_6C_6C_{14}][Tf_2N]$ is much larger than [bmim][BF_4] and the steric effect may not be ignored.

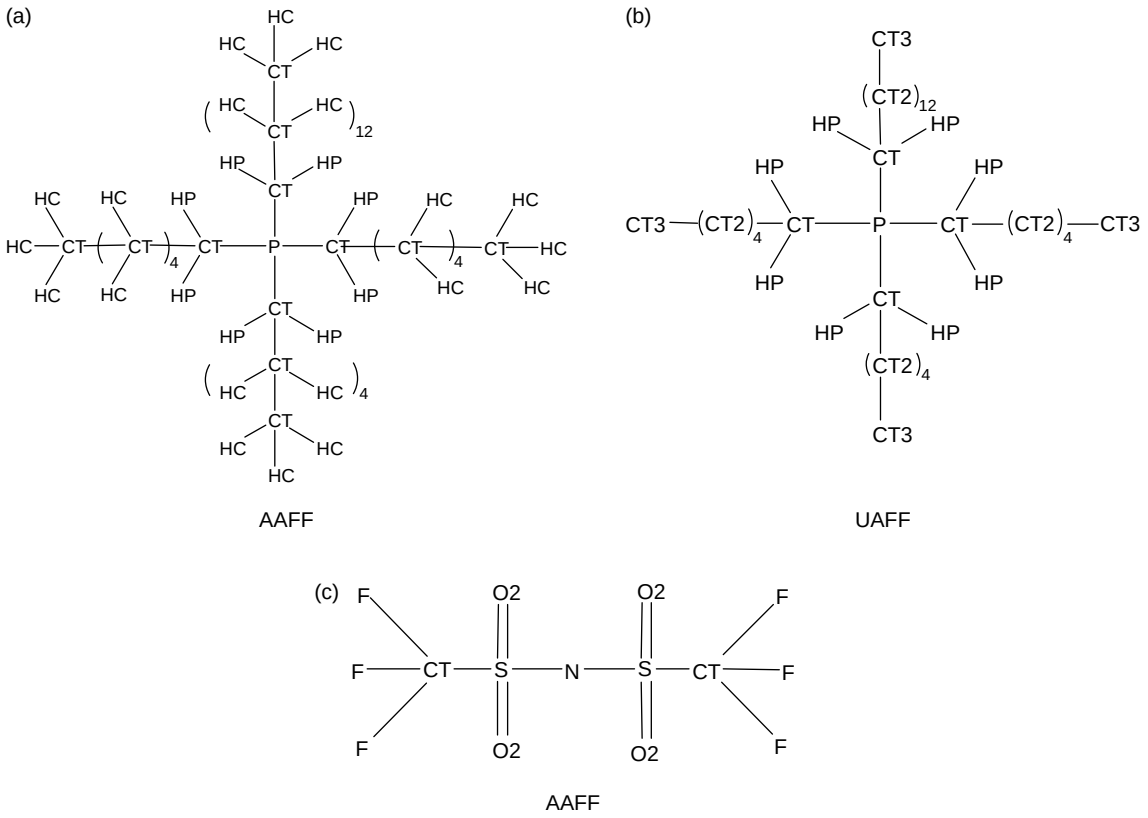

Figure 2. Molecular structures and atom types for $[PC_6C_6C_6C_{14}]^+$ and $[Tf_2N]^-$. (a) AAFF, (b) UAFF, (c) AAFF.

As a result, we preferred the AAFF to the UAFF in the following parts.

These are two possible reasons for the differences between the simulated and the experimental data. The anion force fields may not be sufficient to accurately represent the distribution of charges in the real systems. It is also found that simulated densities and experimental results for the ILs composed of ions with some polar atoms, just like Tf_2N^-, are usually not fitted very well, as our previous work proved [14]. Another crucial reason is that the Lennard-Jones potential may not be realistic enough to describe interactions within these systems accurately, especially for hydrogen bonding.

The internal energies *U* were also calculated. As is shown in Figure 4, we find that the UAFF internal energies are all smaller than the AAFF ones. It may be caused by the fact that the UAFF treats several atoms as a single interaction centre, and that part of the total energy was omitted. It is obvious that *U* increases linearly with increasing temperature. Based on the internal energy, heat

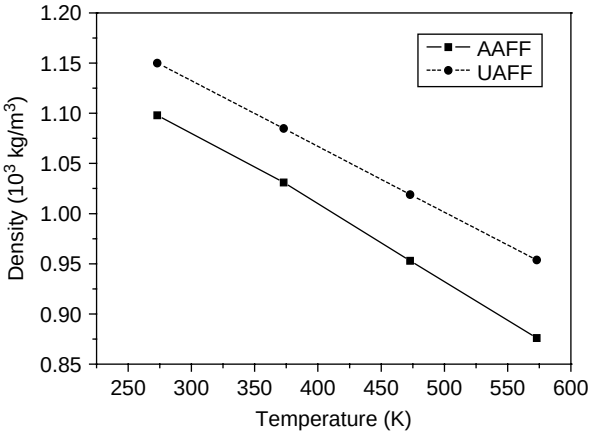

Figure 3. Liquid densities based on the two force fields.

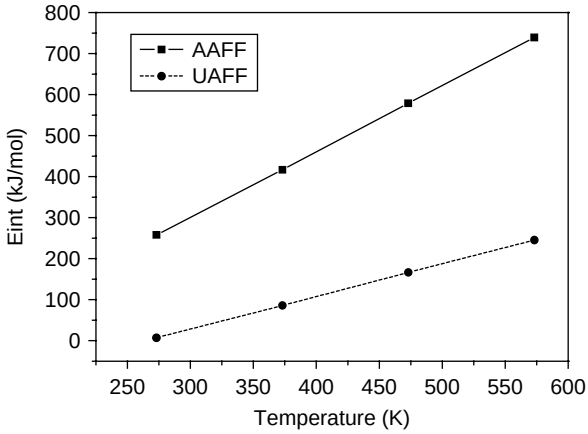

Figure 4. Liquid internal energies based on the two force fields.

capacities at constant pressure were also obtained using the estimation equation as below [28],

$$C_p(T,p) = \left(\frac{\partial H}{\partial T}\right)_p \approx \left[\frac{H(T+\Delta T) - H(T)}{\Delta T}\right]_p, \quad (1)$$

where H is the enthalpy, and it can be calculated by

$$H = U + pV. \quad (2)$$

Thus, the C_p between 273 and 573 K is 1.606 kJ/mol/K or 2.078 J/g/K based on AAFF.

3.2 Transport properties

It is known that ILs can be used in extensive fields. However, one of the bottlenecks is the sluggish dynamics properties [6,29,30]. Designing task-specific ILs with lower viscosities is important for both scientific research and industrial technology. In this work, we studied the SDCs, viscosities, and conductivities to explore the dynamics properties of $[PC_6C_6C_6C_{14}][Tf_2N]$.

The translational SDCs can be determined by two methods: mean square displacement (MSD) or velocity autocorrelation functions. In this work, the SDCs were obtained using the Einstein relation (Equation (3)) [6] based on the MSDs recorded with the interval of 0.1 ps. The start point and time region to a linear fit of MSD are different from each other in the reported work [31,32], and it is said that fitting should avoid the initial and final regions [33]. Consequently, trajectories were dumped for 4.0 ns at 273 K and the range 500–3000 ps was used for estimating the slope by linear regression. At the other three temperatures, the range 500–1500 ps was used. The evolution of the MSDs over time is plotted in Figure 5. After skipping over the short-term nonlinearity in the first

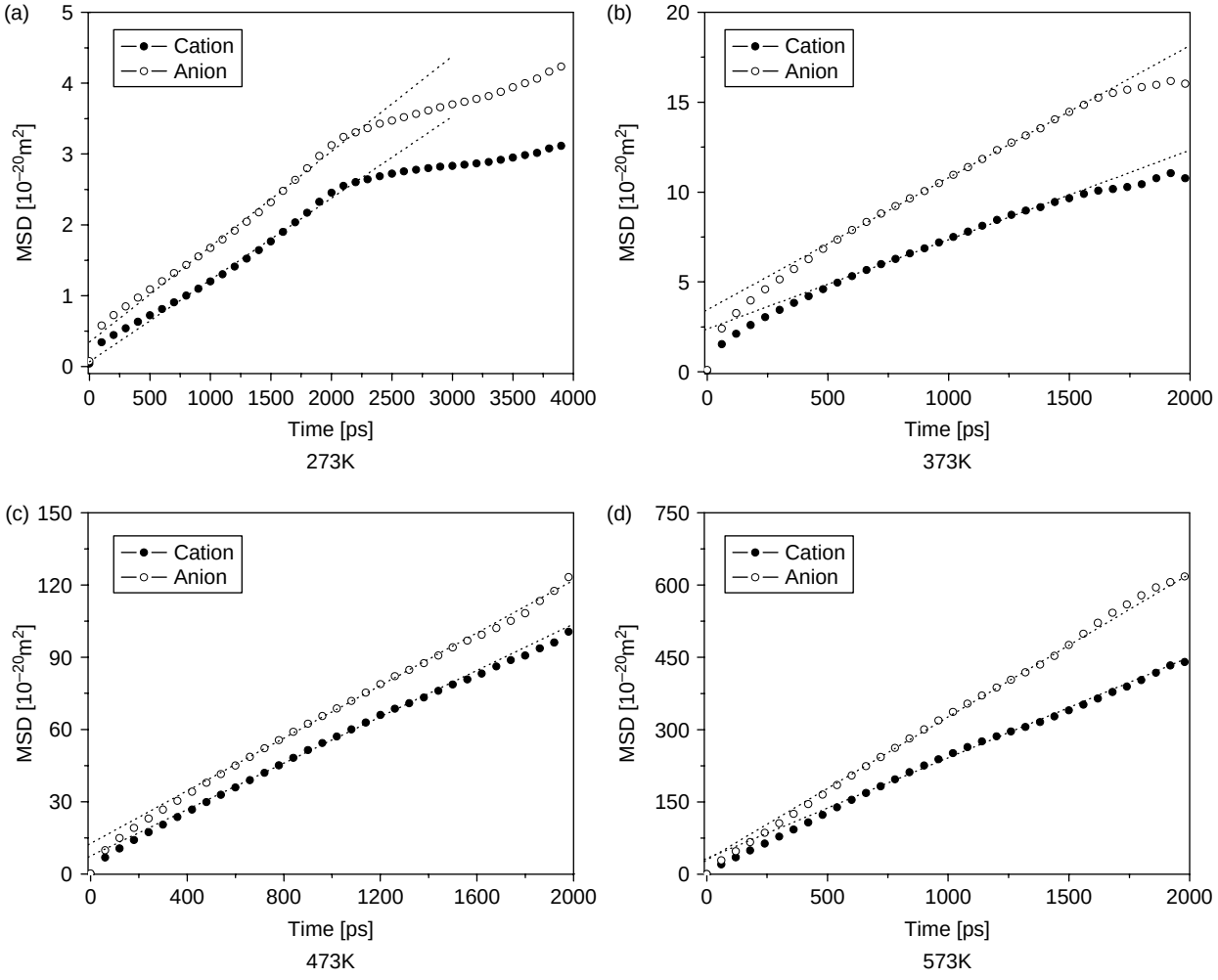

Figure 5. Average mean square displacements of $[PC_6C_6C_6C_{14}][Tf_2N]$. (a) 273 K, (b) 373 K, (c) 473 K, (d) 573 K.

few pico seconds, a sub-diffusive regime with good linearity was observed.

$$D_{\text{self}} = \frac{1}{6}\lim_{t\to\infty}\frac{\mathrm{d}}{\mathrm{d}t}\langle|r_i(t) - r_i(0)|\rangle. \quad (3)$$

In order to make a comparison more clearly, the SDCs for cations, anions and ILs are all shown in Figure 6. As expected, all the diffusion coefficients increase and the increase velocities become faster at the higher temperature. $[Tf_2N]^-$ is found to move faster than $[PC_6C_6C_6C_{14}]^+$, and that may be caused by the smaller volume and freer transfer of $[Tf_2N]^-$.

Viscosities η_{IL}, molar conductivities Λ_{IL} and conductivities κ_{IL} were all obtained based on the corresponding equation listed below [8,34],

$$\eta_{\text{IL}} = \eta_{\text{H}_2\text{O}}\frac{D_{\text{H}_2\text{O}}}{D_{\text{IL}}}, \quad (4)$$

$$\Lambda_{\text{IL}} = \frac{N_\Lambda e^2}{k_{\text{B}}T}(D_{\text{cation}} + D_{\text{anion}}), \quad (5)$$

$$\kappa_{\text{IL}} = \Lambda_{\text{IL}} \times (\rho/M) \quad (6)$$

and the results are presented in Table 1. For D_{IL}, it can be calculated by 1/2 $(D_{\text{cation}} + D_{\text{anion}})$. Compared with the viscosity of water, which is 0.9 mPa s [35], it is obvious that the IL moves very slowly, especially at low temperatures.

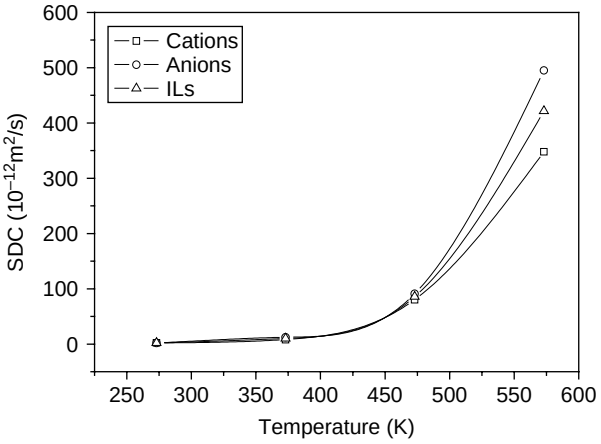

Figure 6. Self-diffusion coefficients of $[PC_6C_6C_6C_{14}][Tf_2N]$.

Table 1. Transport properties of $[PC_6C_6C_6C_{14}][Tf_2N]$.

T (K)	D_{IL} (10^{-12} m^2/s)	η_{IL} (10^{-3} Pa s)	Λ_{IL} (10^{-4} S m^2/mol)	κ_{IL} (10^{-2} S/m)
273	2.08	994.24	0.17	0.02
293	2.81	735.74	0.20	0.03
373	10.27	201.54	0.62	0.07
473	85.71	24.15	3.68	0.47
573	421.44	4.91	14.96	3.83

It is reported [17] that the viscosity is 450 cP for $[PC_6C_6C_6C_{14}][Tf_2N]$ at 293 K. In order to test the proposed force field, the MSD at 293 K was also recorded with the interval of 0.1 ps for 2.0 ns. Based on the MSD, the SDF and viscosity were obtained and are shown in Table 1. Compared with experimental data, it seems that the error is unacceptable. However, the transport properties are always difficult to predict exactly. The biggest problem is the computed time: as most of the ILs move very slowly, it is difficult to obtain data in good agreement with the experiment in a short period, e.g. several nanoseconds. Another factor may be the purity of the product. It is impossible to remove the impurities thoroughly in a sample, and sometimes trace amounts of impurities such as water can change the value of the viscosity dramatically [36]. For example, the experimental viscosities for $BmimPF_6$ are reported to be 207 [37], 273 [38] and 450 cP [39] at 293 K, respectively. Based on the simulated SDFs being 3.5×10^{-12} [33] and 11×10^{-12} m^2/s [40], and according to Equation (4), the corresponding viscosities are 591.43 and 188.18 cP, respectively.

RDFs between cations and anions at different temperatures were studied in order to analyse the reason for high viscosities. It is reported that the hydrogen bond could be found between anions and HP in cations [16]; thus the interactions between the HP with C, F and etc. were investigated. No matter whether the HP belongs to hexyl or tetradecyl, differences can be found. Consequently, only the RDFs for HP in tetradecyl are shown in Figure 7. It is observed from Figure 7(a) that interaction strength between HP in cations and O atom in anions is strong (473 K), and hydrogen bonds may exist. In order to investigate the temperature influence, the H—O RDFs at the four temperatures are shown in Figure 7(b). It is obvious that the interaction becomes weaker with increasing temperature. The above results could be used to explain the high viscosity at normal temperature and lower viscosity at higher temperature.

3.3 Radial distribution functions

In order to analyse the organisation of the bulk, centre-of-mass RDFs for cation–anion, anion–anion, cation–cation and also the P—P RDFs at 473 K were first discussed. As is shown in Figure 8(a), the association between cation–anion and anion–anion is obvious. However, the solvent shells of cation–cation and the P atoms around themselves are nearly impossible to find. This may be an implication that the interaction of cations is complex, and the aggregation of cations may have some effect on the distribution [41]. Centre-of-mass RDFs for cation–anion and anion–anion at different temperatures are shown in Figure 8(b). The solvent shells for anions around cations and anions around anions expanded a little temperature with increasing. After integrating the RDFs from zero

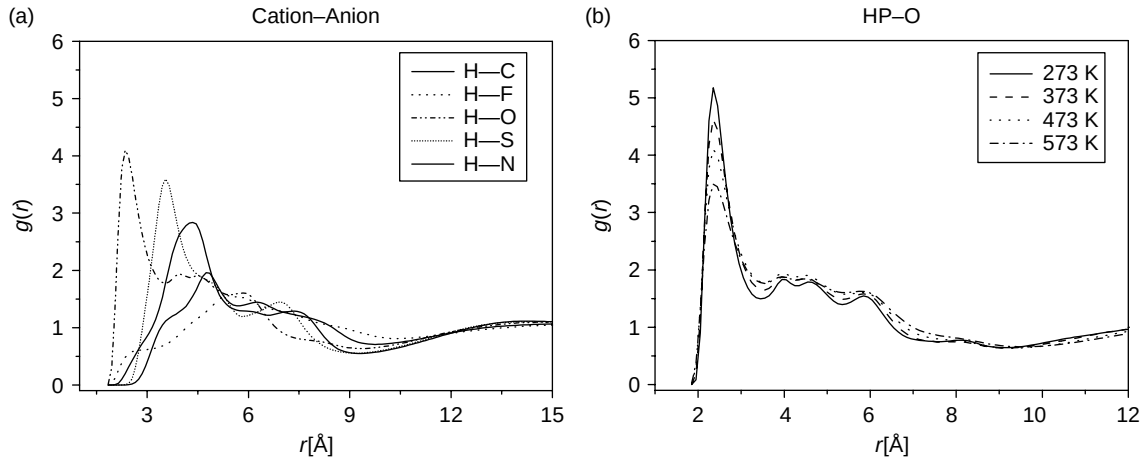

Figure 7. Site-to-site RDFs of $[PC_6C_6C_6C_{14}][Tf_2N]$. (a) cation–anion, (b) HP–O.

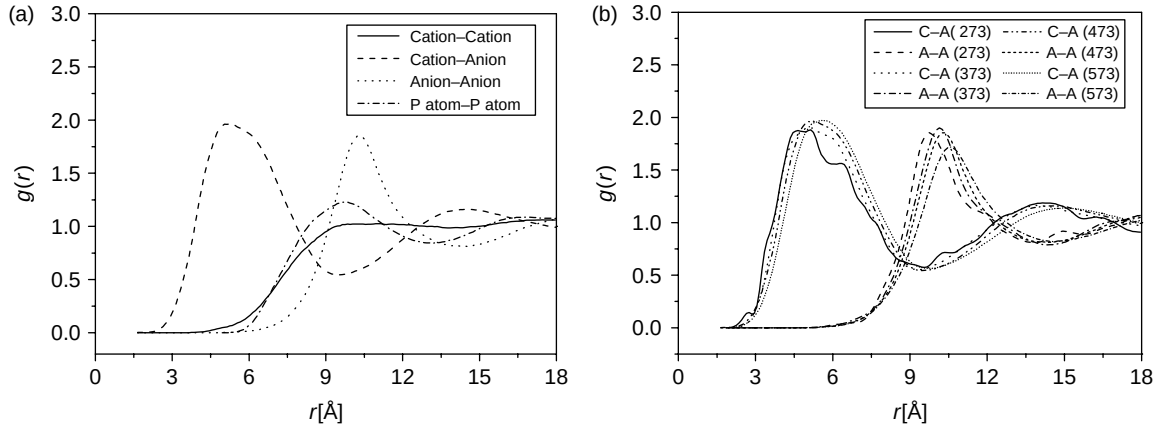

Figure 8. Centre-of-mass RDFs of $[PC_6C_6C_6C_{14}][Tf_2N]$.

to the first minimum, we obtained the coordination numbers in the first solvent shell. The coordination number N can be calculated by [40]

$$N = 4\pi\int_0^{R_{\min 1}} \rho g(r) r^2 \mathrm{d}r \qquad (7)$$

where ρ is the number density. It is found that each cation is surrounded by about three anions in the first solvent shell.

3.4 Spatial distribution functions

More intuitive structures were obtained from the SDFs, which give the probability of finding an atom in the three-dimensional space around a centre molecule, in contrast to the average values given by RDF [40]. SDFs visualised by the software package gOpenMol [42] are shown in Figure 9, and the red and yellow contour surfaces are drawn at 20 and 6 times of the average density. It is obvious that the probability distribution of the anion is around the alkyl of the cation, and hydrogen bonds may exist in the red region. As is seen in the figure, the red regions become smaller in the order of 273 K $>$ 373 K $>$ 473 K, and nearly no red region is observed in Figure 9(d). It is evident that the interaction between cation and anion becomes weaker with increasing temperature.

4. Conclusions

In this work, a kind of phosphonium-based IL $[PC_6C_6C_6C_{14}][Tf_2N]$ was studied by molecular dynamics simulation based on both AAFF and UAFF. It is found that simulated densities decrease and internal energies increase linearly with increasing temperature. Compared with the experimental density, the AAFF result is proved to be much more reliable. The SDC, viscosities, and conductivities were investigated to explore the dynamics properties of $[PC_6C_6C_6C_{14}][Tf_2N]$. It is observed that all the SDCs increase and that the increase in velocities becomes faster when the temperature becomes higher. RDFs were utilised to analyse the reason for the high viscosity at normal temperature and lower viscosity at higher temperature, and

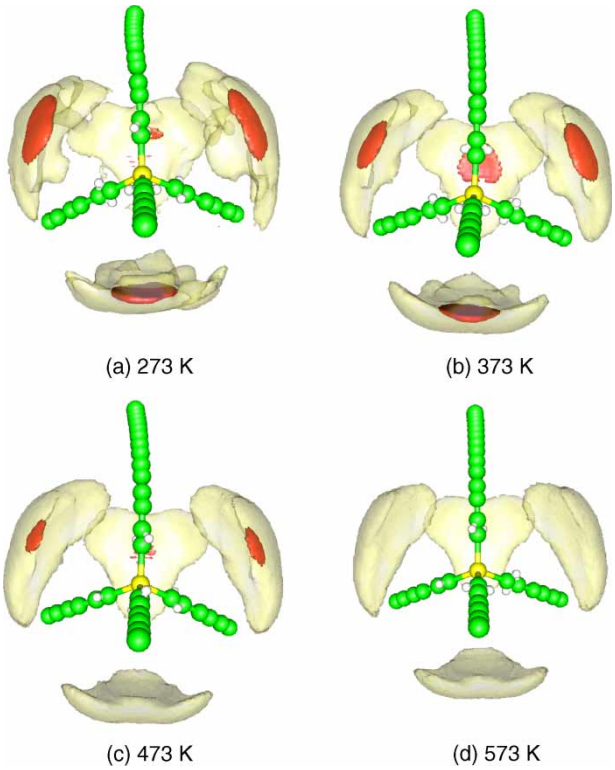

Figure 9. Spatial distribution functions for $[PC_6C_6C_6C_{14}][Tf_2N]$. Red and yellow contour surfaces are drawn at 20 and 6 times of the average density. (a) 273 K, (b) 373 K, (c) 473 K, (d) 573 K.

it is found that HP in cations and O in anions could form hydrogen bonds. Integrating the centre-of-mass RDFs, we observe that each cation is surrounded by about three anions in the first solvent shell. The visualised pictures of the SDFs show intuitively the three-dimensional probability distribution of the anion around the central cation. It is also found that interaction between ions becomes weaker with increasing temperature.

Acknowledgements

This work was supported by the National Science Fund of China for Distinguished Young Scholar (20625618), National Basic Research Program of China (2009CB219902), Knowledge Innovation Program of the Chinese Academy of Sciences (KGCX2-YW-321) and National Natural Scientific Fund of China (20603040).

References

[1] C. Cadena, J.L. Anthony, J.K. Shah, T.I. Morrow, J.F. Brennecke, and E.J. Maginn, *Why is CO_2 so soluble in imidazolium-based ionic liquids?*, J. Am. Chem. Soc. 126 (2004), pp. 5300–5308.

[2] C.G. Hanke and R.M.J. Lynden-Bell, *A simulation study of water-dialkylimidazolium ionic liquid mixtures*, J. Phys. Chem. B 107 (2003), pp. 10873–10878.

[3] M.G.D. Popolo and G.A. Voth, *On the structure and dynamics of ionic liquids*, J. Phys. Chem. B 108 (2004), pp. 1744–1952.

[4] J.N.C. Lopes and A.A.H. Pádua, *Nanostructural organization in ionic liquids*, J. Phys. Chem. B 110 (2006), pp. 3330–3335.

[5] J.N.C. Lopes and A.A.H. Pádua, *Molecular force field for ionic liquids composed of triflate or bistriflylimide anions*, J. Phys. Chem. B 108 (2004), pp. 16893–16898.

[6] T.I. Morrow and E.J. Maginn, *Molecular dynamics study of the ionic liquid 1-n-Butyl-3-methylimidazolium hexafluorophosphate*, J. Phys. Chem. B 106 (2002), pp. 12807–12813.

[7] J.d. Andrade, E.S. Bo1es, and H. Stassen, *A force field for liquid state simulations on room temperature molten salts: 1-ethyl-3-methylimidazolium tetrachloroaluminate*, J. Phys. Chem. B 106 (2002), pp. 3546–3548.

[8] C.J. Margulis, H.A. Stern, and B.J. Berne, *Computer simulation of a 'green chemistry' room-temperature ionic solvent*, J. Phys. Chem. B 106 (2002), pp. 12017–12021.

[9] M. Bühl, A. Chaumont, R. Schurhammer, and G. Wipff, Ab initio *molecular dynamics of liquid 1,3-dimethylimidazolium chloride*, J. Phys. Chem. B 109 (2005), pp. 18591–18599.

[10] http://159.226.63.142/gct/menu.htm

[11] J.F. Brennecke and E.J. Maginn, *Ionic liquids: Innovative fluids for chemical processing*, AIChE J. 47 (2001), pp. 2384–2389.

[12] R. Brookes, A. Davies, G. Ketwaroo, and P.A. Madden, *Diffusion coefficients in ionic liquids: Relationship to the viscosity*, J. Phys. Chem. B 109 (2005), pp. 6485–6490.

[13] X. Liu, G. Zhou, S. Zhang, G. Wu, and G. Yu, *Molecular simulation of guanidinium-based ionic lliquids*, J. Phys. Chem. B 111 (2007), pp. 5658–5668.

[14] X. Liu, S. Zhang, G. Zhou, G. Wu, X. Yuan, and X. Yao, *New force field for molecular simulation of guanidinium-based ionic liquids*, J. Phys. Chem. B 110 (2006), pp. 12062–12071.

[15] J. McNulty, J.J. Nair, S. Cheekoori, V. Larichev, A. Capretta, and A.J. Robertson, *Scope and mechanistic insights into the use of tetradecyl(trihexyl)phosphonium bistriflimide: A remarkably selective ionic liquid solvent for substitution reactions*, Chem. Eur. J. 12 (2006), pp. 9314–9322.

[16] G.H. Zhou, X.M. Liu, S.J. Zhang, G.G. Yu, and H.Y. He, *A force field for molecular simulation of tetrabutylphosphonium amino acid ionic liquids*, J. Phys. Chem. B 111 (2007), pp. 7078–7084.

[17] R.E.D. Sesto, C. Corley, A. Robertson, and J.S. Wilkes, *Tetraalkylphosphonium-based ionic liquids*, J. Org. Chem. 690 (2005), pp. 2536–2542.

[18] J.N.C. Lopes and A.A.H. Pádua, *Molecular force field for ionic liquids III: Imidazolium, pyridinium, and phosphonium cations; chloride, bromide, and dicyanamide anions*, J. Phys. Chem. B 110 (2006), pp. 19586–19592.

[19] W.D. Cornell, P. Cieplak, C.I. Bayly, I.R. Gould, K.M. Merz, D.M. Ferguson, D.C. Spellmeyer, T. Fox, J.W. Caldwell, and P.A. Kollman, *A second generation force field for the simulation of proteins, nucleic acids, and organic molecules*, J. Am. Chem. Soc. 117 (1995), pp. 5179–5197.

[20] J.N.C. Lopes and A.A.H. Pádua, *Molecular force field for ionic liquids composed of triflate or bistriflylimide anions*, J. Phys. Chem. B 108 (2004), pp. 16893–16898.

[21] T. Fox and P.A. Kollman, *Application of the RESP methodology in the parameterization organic solvents*, J. Phys. Chem. B 102 (1998), pp. 8070–8079.

[22] W.D. Cornell, P. Cieplak, C.I. Bayly, and P.A. Kollmann, *Application of RESP charges to calculate conformational energies, hydrogen bond energies, and free energies of solvation*, J. Am. Chem. Soc. 115 (1993), pp. 9620–9631.

[23] P. Cieplak, W.D. Cornell, C. Bayly, and P.A. Kollman, *Application of the multimolecule and multiconformational RESP methodology to biopolymers: Charge derivation for DNA, RNA, and proteins*, J. Comput. Chem. 16 (1995), pp. 1357–1377.

[24] J.M. Wang, P. Cieplak, and P.A. Kollman, *How well does a restrained electrostatic potential (RESP) model perform in calculating conformational energies of organic and biological molecules?*, J. Comput. Chem. 21 (2000), pp. 1049–1074.

[25] A.P. Lyubartsev and A. Laaksonen, *M.DynaMix - A scalable portable parallel MD simulation package for arbitrary molecular mixtures*, Comput. Phys. Commun. 128 (2000), pp. 565–589.

[26] G.J. Martyna, M.E. Tuckerman, D.J. Tobias, and M.L. Klein, *Explicit reversible integrators for extended systems dynamics*, Mol. Phys. 87 (1996), pp. 1117–1157.
[27] X. Wu, Z. Liu, S. Huang, and W. Wang, *Molecular dynamics simulation of room-temperature ionic liquid mixture of [Bmim][BF4] and acetonitrile by a refined force field*, Phys. Chem. Chem. Phys. 7 (2005), pp. 2771–2779.
[28] M. Lagache, P. Ungerer, A. Boutina, and A.H. Fuchsa, *Prediction of thermodynamic derivative properties of fluids by Monte Carlo simulation*, Phys. Chem. Chem. Phys. 3 (2001), pp. 4333–4339.
[29] C. Cadena, Q. Zhao, R.Q. Snurr, and E.J. Maginn, *Molecular modeling and experimental studies of the thermodynamic and transport properties of pyridinium-based ionic liquids*, J. Phys. Chem. B 110 (2006), pp. 2821–2832.
[30] C. Cadena and E.J. Maginn, *Molecular simulation study of some thermophysical and transport properties of triazolium-based ionic liquids*, J. Phys. Chem. B 110 (2006), pp. 18026–18039.
[31] M. Fioroni, K. Burger, A.E. Mark, and D.J. Roccatano, *A new 2,2,2-trifluoroethanol model for molecular dynamics simulations*, J. Phys. Chem. B 104 (2000), pp. 12347–12354.
[32] P. Ren and J.W. Ponder, *Polarizable atomic multipole water model for molecular mechanics simulation*, J. Phys. Chem. B 107 (2003), pp. 5933–5947.
[33] N.M. Micaelo, A.M. Baptista, and C.M. Soares, *Parametrization of 1-butyl-3-methylimidazolium hexafluorophosphate/nitrate ionic liquid for the GROMOS Force Field*, J. Phys. Chem. B 110 (2006), pp. 14444–14451.
[34] A. Noda, K. Hayamizu, and M. Watanabe, *Pulsed-gradient spin-echo ^{1}H and ^{19}F NMR ionic diffusion coefficient, viscosity, and ionic conductivity of non-chloroaluminate room-temperature ionic liquids*, J. Phys. Chem. B 105 (2001), pp. 4603–4610.
[35] C.L. Yaws, J.W. Miller, P.N. Shah, G.R. Schorr, and P.M. Patel, *Correlation constants for chemical compounds*, Chem. Eng. 83 (1976), pp. 153–162.
[36] M.S. Kelkar and E.J. Maginn, *Effect of temperature and water content on the shear viscosity of the ionic liquid 1-ethyl-3-methylimidazolium bis(trifluoromethanesulfonyl)imide as studied by atomistic simulations*, J. Phys. Chem. B 111 (2007), pp. 4867–4876.
[37] N.B. Sheila, A.K. Maureen, and V. Frank, *Bright the cybotactic region surrounding fluorescent probes dissolved in 1-butyl-3-methylimidazolium hexafluorophosphate: Effects of temperature and added carbon dioxide*, J. Phy. Chem. B 105 (2001), pp. 9663–9668.
[38] K.R. Harris and L.A. Woolf, *Temperature and pressure dependence of the viscosity of the ionic liquid 1-butyl-3-methylimidazolium hexafluorophosphate*, J. Chem. Eng. Data 50 (2005), pp. 1777–1782.
[39] J.G. Huddleston, A.E. Visser, W.M. Reichert, H.D. Willauer, G.A. Broker, and R.D. Rogers, *Characterization and comparison of hydrophilic and hydrophobic room temperature ionic liquids incorporating the imidazolium cation*, Green Chem. 3 (2001), pp. 156–164.
[40] Z. Liu, S. Huang, and W. Wang, *A refined force field for molecular simulation of imidazolium-based ionic liquids*, J. Phys. Chem. B 108 (2004), pp. 12978–12989.
[41] X. Liu, G. Zhou, X. Yao, and S. Zhang, *Nano-structure and behavior in phosphonium-based ionic liquid*, Chem. Commun. (2009), submitted.
[42] L. Laaksonen, *A graphics program for the analysis and display of molecular-dynamics trajectories*, J. Mol. Graph. 10 (1992), pp. 33–34.